JOURNAL OF MATERIALS SCIENCE 26 (1991) 6331–6340

Correlation between the mechanical properties and microstructural changes of aged Al–5.8% Mg alloy

A. M. HAMMAD*, M. A. SHABAN, S. M. SHERIF
Materials Science Division, Physics Department, Tajura Nuclear Research Centre, Atomic Energy, P. O. Box 397, Tripoli, Libya

Mechanical properties of aged Al–5.8% Mg alloy at 423 and 473 K, over the ageing time range 1–35 h, have been investigated to assess the effect of ageing temperature on deformation in the presence of precipitation. The results indicate that the 0.2% yield strength, ultimate tensile strength, flow stress, work hardening exponent and ductility increase with ageing time reaching a maximum value, and then decrease to minimum value, followed by an increase at longer ageing times. The variation in yield, ultimate tensile strength, work hardening exponent of the flow, as well as the hardness at different degrees of deformation, were recorded as functions of experimental variables. Electron microscopic investigations revealed that the strengthening and loss in ductility of the alloy may be attributed to the precipitation of different shapes of $MnAl_6$, Mg_2Al_3 and ε-$Mg_{23}Al_{30}$, whose size, quantity and morphology depend on the experimental conditions. An attempt has been made to correlate strength, ductility and structural changes at different ageing times. The Brinell hardness increases and the recrystallization temperature decreases with deformation. From parabolic stress–strain relation, the σ–$\varepsilon^{1/2}$ curves could be divided into two linear parts.

1. Introduction

The most important aspect of any engineering material is its structure, because its properties are closely related to this feature. To be successful, materials engineers must have a good understanding of the relationship between structure and properties. Several commercially important aluminium alloy systems have been subjected to careful investigation of the structures existing at various stages of the precipitation process. As such, alloying elements are usually added to aluminium to increase its strength, although improvement in other properties is very important. Research and development in the field of aluminium alloys, particularly of the high-strength, age-hardening types, therefore occupy a position of importance. Intensive research over many decades has resulted in a progressive accumulation of knowledge concerning the atomic and crystallographic structural changes, that occur in supersaturated solid solutions during precipitation and the mechanisms through which the structure forms and alters alloy properties. In most precipitation-hardenable systems, a complex sequence of time- and temperature-dependent changes is involved. No element is known to have complete miscibility with aluminium in the solid state. The Al–Mg family of alloys are the simplest and owe their strength solely to their marked work-hardening response which increases with magnesium content [1]. The other alloys are all dependent for their highest strengths on artificial ageing giving precipitation of crystallographically coherent, metastable, forms of intermetallic phases. In order to develop this type of hardening, special conditions of precipitate nucleation are necessary, together with a practical possibility of supersaturation of the solute, so that useful amounts of hardening precipitate can be produced. This accounts for the limited number of these heat-treatable alloy systems. The age-hardening process also involves atomic rearrangements accompanying the breakdown of the supersaturated solid solution. This occurs by diffusional, nucleation and growth processes. The relative rates at which solution and precipitation reactions occur with different solutes, depend on the respective diffusion rates, in addition to solubilities and alloying contents. The rate of growth of the nuclei is controlled by the rate of atomic migration in the alloy. Thus the ageing temperature has a pronounced effect. Moreover, the increase in the strength of the alloy depends on the structure, spacing, size, shape and distribution of the precipitated particles, as well as on the degree of structural and crystallographic coherency with the matrix. Thus, studies concerning structure–property correlations and the development of methods of improving the

* *Permanent address*: The Atomic Energy Establishment, Metallurgy Department, Cairo, Egypt.

0022–2461/91 $03.00 + .12

strength of the materials without a significant loss of ductility constitute relevant research of technological significance. The variations in strength and ductility with deformation temperature have been studied for commercial grade aluminium, Al–Ge, Al–Si, Al–Fe, Al–Zn, Al–Cu, Al–Mg and for different materials, and have been correlated separately with structural changes [2–14].

In the present investigation, the room-temperature tensile deformation behaviour of Al–5.8% Mg alloy aged for different times at 423 and 473 K has been investigated. The variations in the properties have been correlated with the microstructural changes accompanying the deformation of aged material.

2. Experimental procedure

The starting material was in the form of cylindrical shapes with the chemical composition given in Table I.

Tensile specimens, with the dimensions 15 mm × 3 mm × 1 mm, were die-stamped from 1 mm thick strips, obtained from hot-rolled discs of 50 mm diameter and 5 mm thickness, into 1 mm thick sheets. The tensile axes were parallel to the rolling direction. Slight surface irregularities introduced by rolling were removed by chemical etching. Only specimens without surface flows were considered for tensile tests. Heat treatment carried out before tensile testing consisted of, solution treatment for 2 h at 823 K, water quenched, followed by ageing for different times at 423 and 473 K (isothermal ageing). The grain size, as measured by the linear intercept method, was 25 μm.

Tensile tests were performed at room temperature (293 K) on an Instron tensile testing machine at strain rate of $5.56 \times 10^{-5} s^{-1}$. To ensure the reproducibility of results at each experimental condition, at least two specimens were tested.

To study the effect of different degrees of deformation on the recrystallization temperature, as-received as well as deformed samples of Al–5.8% Mg were isochronally annealed for 1 h at different temperatures and the Brinell hardness was measured.

Gauge portions of the fractured specimens were subjected to electron microscopic investigations for identifying the important features. Thin foils were prepared using a twin-jet electrolytic polisher and a polishing solution of 10% perchloric acid, 20% glycerine and 70% methanol at 268 K. Thin foils were examined in a 100 kV transmission electron microscope fitted with an attachment for X-ray microanalysis at RUCA, University of Antwerp, Belgium.

3. Results

3.1. Mechanical properties

The effect of ageing time on 0.2% yield stress, the ultimate tensile strength and ductility of Al–5.8% Mg alloy, aged at 423 and 473 K, with a grain size of 25 μm and tensile tested at room temperature (293 K) at a strain rate of $5.56 \times 10^{-5} s^{-1}$, is shown in Figs 1–3. To establish that the extrema observed were genuine, for each condition two tests or more were performed. The average ductility was reported as the

TABLE I Chemical composition of the alloy (wt %)

Mg	Mn	Fe	Si	Cu	Ti	Zn	Be	Al
5.8	0.5	0.40	0.40	0.10	0.02	0.20	0.0002	Bal.

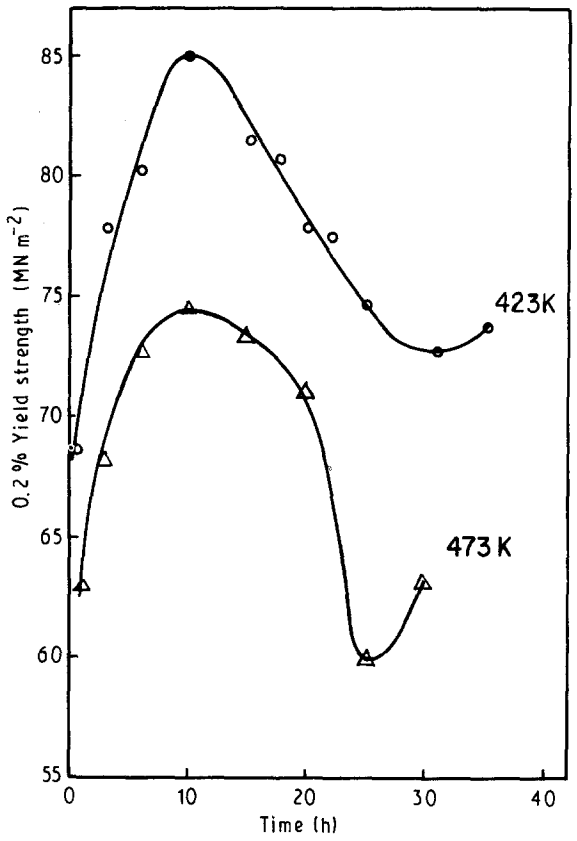

Figure 1 Effect of ageing temperature on 0.2% yield stress versus ageing time. Al-5.8% Mg; $\dot{\varepsilon} = 5.56 \times 10^{-5} S^{-1}$; GS = 25 μm; T = 293 K.

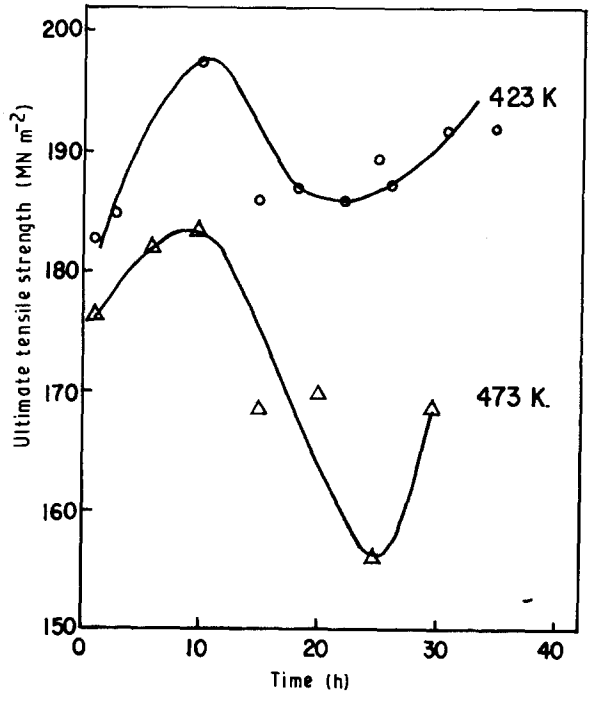

Figure 2 Effect of ageing temperature on the ultimate tensile strength versus ageing time. Al-5.8% Mg; $\dot{\varepsilon} = 5.56 \times 10^{-5} S^{-1}$; GS = 25 μm; T = 293 K.

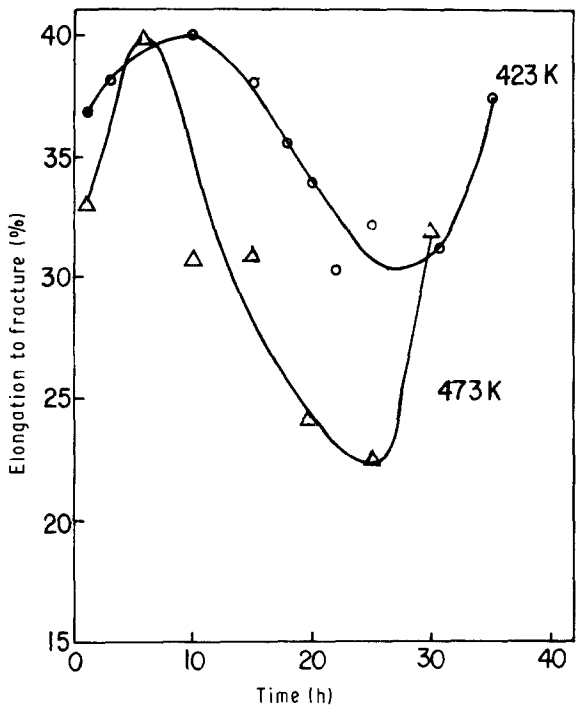

Figure 3 Effect of ageing temperature on the elongation to fracture versus ageing time. Al-5.8% M; $\dot{\varepsilon} = 5.56 \times 10^{-5} S^{-1}$; GS = 25 μm; $T = 293$ K.

elongation to fracture. The results indicate that the ductility increases with ageing time, reaching a maximum value, and then decreases to minimum, followed by an increase at higher ageing time. The ageing time at which the drop in ductility begins depends on the ageing temperature, i.e. the extrema were shifted to the lower ageing time by increasing the ageing temperature (Fig. 3). On the other hand, ductility increases with decreasing ageing temperature.

The variation of 0.2% yield strength and ultimate tensile strength with ageing time is shown in Figs 1 and 2. In general, for specimens aged at 423 and 473 K, an initial increase in yield and ultimate tensile strength is noticed up to 10 h ageing time, followed by a sudden decrease to a minimum value at 31 and 25 h, respectively. Beyond this range, an increase in strength was noticed by increasing the ageing time. On the other hand, higher strength corresponds to the material aged at low temperature.

Stress–strain curves have been used by a number of investigators because of their sensitivity to material and test conditions and the mathematical expression that can be used to represent, analyse and compare them. Fig. 4a–c shows true stress–true strain curves for specimens aged at 423 and 473 K and tensile tested at a strain rate of 5.56×10^{-5} s^{-1}, at 293 K, in the ageing time range 1–35 h. Fig. 4c shows the effect of ageing temperature on the flow stress, which indicates that the flow stress increases with decreasing ageing temperature. The relation between 18% flow stress and ageing time is shown in Fig. 5; this indicates that the behaviour of the curves is similar to that presented in Figs 1 and 2.

According to Ludwic's [15] equation, $\sigma = K\varepsilon^n$, where σ is the true stress, ε is true strain, K a material constant, and n, the work hardening exponent, every stress–strain curve becomes s-shaped and possesses a yield stress and a saturation stress, because the slope $d \log \sigma / d \log \varepsilon$ at low and high strains becomes zero. Around the inflection point, the curve can be approximated by a straight line in which the slope gives the value of n. In the present work, n was evaluated as the slope of $\log \sigma$ versus $\log \varepsilon$, for aged specimens tensile tested at different times, e.g. Fig. 6 presents $\log \sigma$ versus $\log \varepsilon$ at 15 h. The strain hardening index, n, corresponding to the material tensile tested at various conditions is plotted versus ageing time in Fig. 7, and indicates that the work hardening index, n, increases with decreasing aging temperature.

In general, the above results indicate that at constant strain rate, the flow stress (Fig. 4a–c), 18% flow stress (Fig. 5) and the work hardening index, n (Fig. 7), as well as 0.2% yield strength (Fig. 1) and ultimate tensile strength (Fig. 2) increase with ageing time, reach a maximum value and then decrease to a minimum, followed by an increase beyond 25 h. The time at which the drop in the work hardening index, n, starts and/or the minimum value of n, depends on the ageing temperature, i.e. an increase in ageing temperature shifts the maximum and minimum value of n to the lower ageing time.

Following earlier work [2, 5, 6, 9–11], the true stress was plotted versus (true strain)$^{1/2}$ (Fig. 8). As before, it was necessary to divide the total range into two linear portions of different slopes.

In order to study the effect of different degrees of deformation on the recrystallization temperature of Al–5.8% Mg alloy, Brinell hardness tests were carried out on isochronally annealed material at different temperatures (Fig. 9). The curves show that for the deformed material, the hardness increases with increasing degree of deformation. In the temperature range below 625 K, higher hardness is due to deformed material compared to the as-received one, and vice versa above that temperature. The results also show a recovery peak at 375 K for both deformed and as-received material. The recrystallization temperature decreases, as is conventionally known, with deformation.

3.2. Transmission electron microscopy

Both isothermally aged specimens at 423 and 473 K and tensile tested at room temperature, display similar strength and ductility time curves with a time-dependent minimum for each condition (Figs 1–5). Electron microscopic investigations for correlating the observed changes in mechanical properties with microstructure at different ageing times were carried out. No evidence for Guinier–Preston (GP) zone formation could be obtained in either case. Table II shows the change brought about by ageing and deformation at room temperature.

4. Discussion

The basic requirement for an alloy to acquire high strength through heat treatment is that it should undergo a phase transformation or structural change

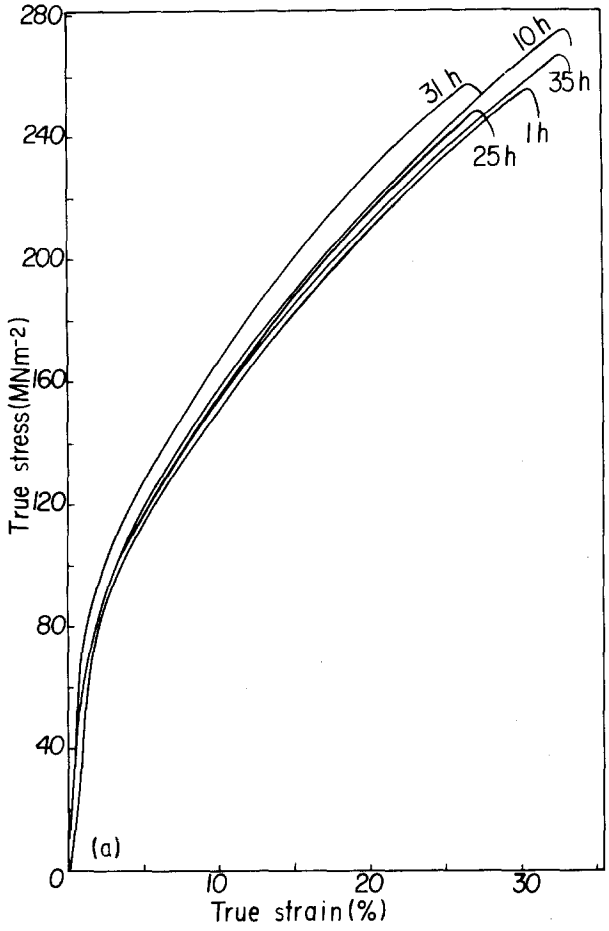

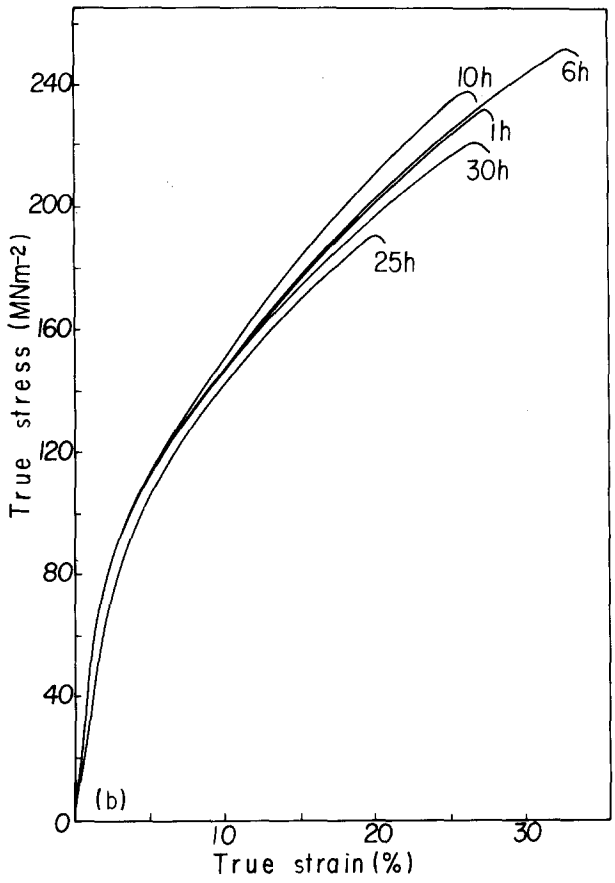

Figure 4 True stress–true strain relation at various ageing times for the material aged at (a, c) 423 and (b) 473 K. Al-5.8 Mg; $\dot{\varepsilon} = 5.56 \times 10^{-5} S^{-1}$; GS = 25 μm; $T = 293$ K.

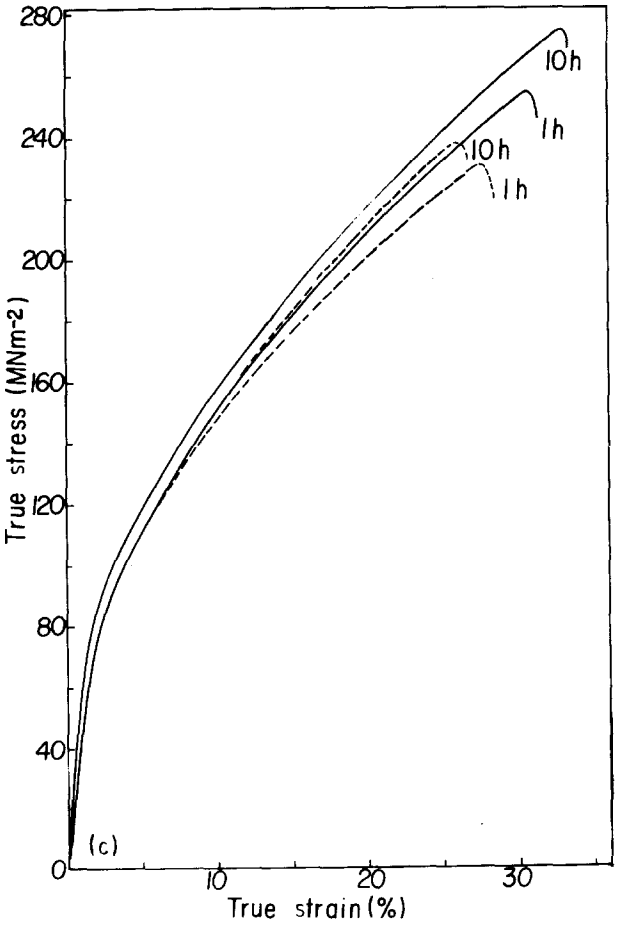

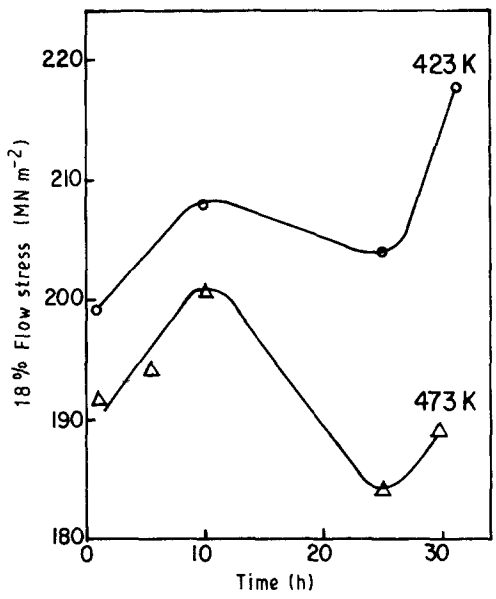

Figure 5 18% Flow stress versus ageing time. Al-5.8 Mg; $\dot{\varepsilon} = 5.56 \times 10^{-5} S^{-1}$; GS = 25 μm; $T = 293$ K.

in the solid state. The precipitation reaction is the most widely investigated in this connection. The precipitation process in aluminium alloys responsible for age hardening at relatively low temperatures (in the vicinity of the ambient), is governed by a thermally activated enhanced diffusion mechanism, due to the presence of quenched-in vacancies in the supersaturated solid solution. The chemical composition of the alloy, state of deformation, ageing temperature and

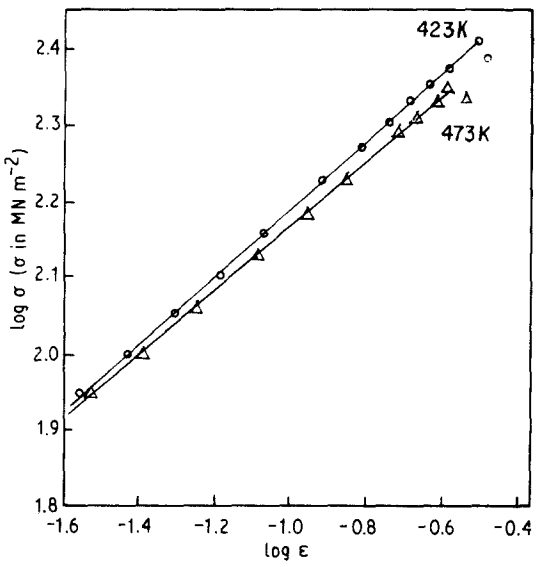

Figure 6 Log (true stress) versus log (true strain) at an ageing time of 15 h, $\dot{\varepsilon} = 5.56 \times 10^{-5}\,s^{-1}$, $T = 293$ K.

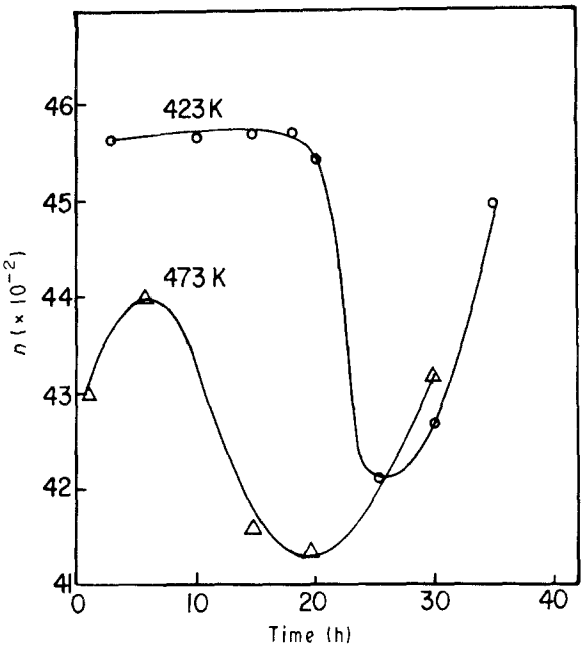

Figure 7 The strain hardening exponent, n, as a function of ageing time. $\dot{\varepsilon} = 5.56 \times 10^{-5}\,s^{-1}$, $T = 293$ K.

ageing time, exert a profound influence on the ultimate mechanical and physical properties of the alloy. A condition for the hardening process to occur, is the precipitation of particles from an aluminium-based supersaturated solid solution. The increase in strength and hardness depends largely on the structure, spacing, size, shape and distribution of the precipitated particles, as well as on the degree of structural and crystallographic coherency with the matrix. In general, plastic deformation of an aluminium alloy is usually associated with an increase in dislocation content. The nature and distribution of the resulting substructure depends on the extent, temperature and time of ageing, rate of deformation and also on other microstructural conditions, such as grain size, particle size and distribution.

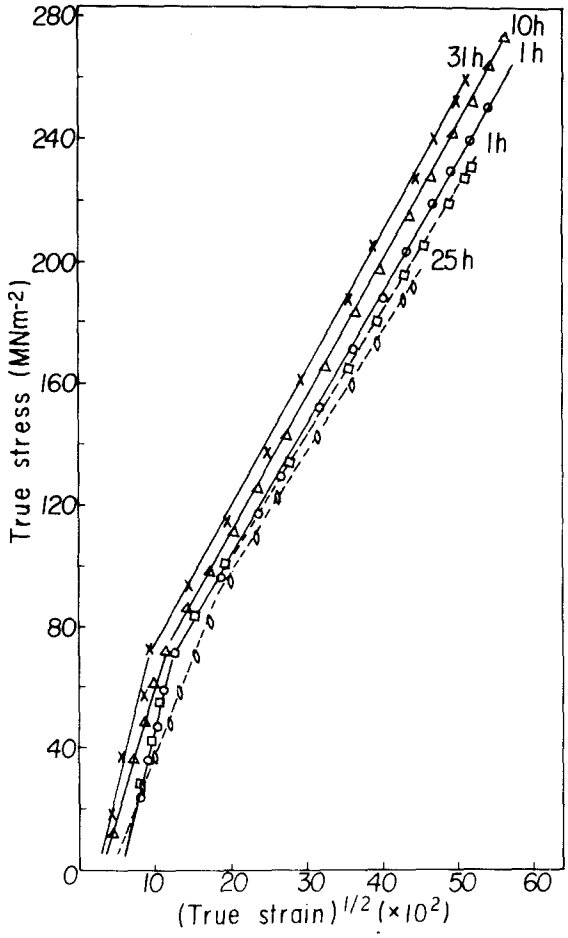

Figure 8 True stress versus (true strain)$^{1/2}$ at various ageing times, and aged at (—) 423 K, (– – –) 473 K.

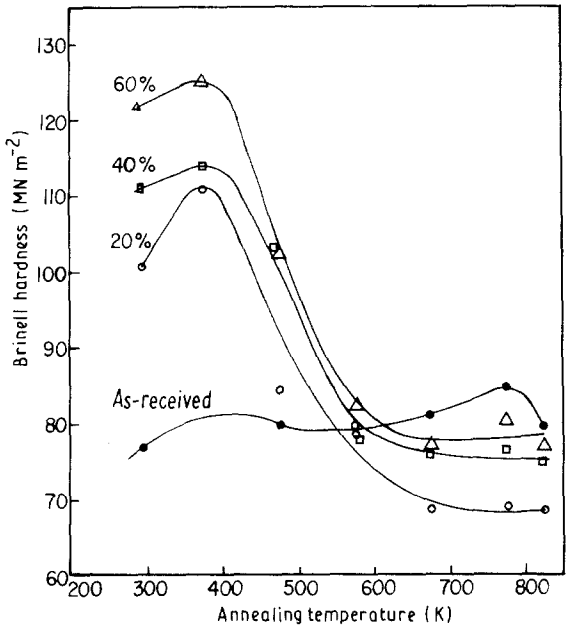

Figure 9 Effect of deformation on Brinell hardness versus annealing temperature (isochronal annealing curves).

The results of the present work have shown that the shape of the 0.2% yield strength (Fig. 1), ultimate tensile strength (Fig. 2), flow stress (Figs 4, 5), work hardening exponent, n (Fig. 7), and ductility (Fig. 3)–time curves is the same, i.e. in both isothermally aged

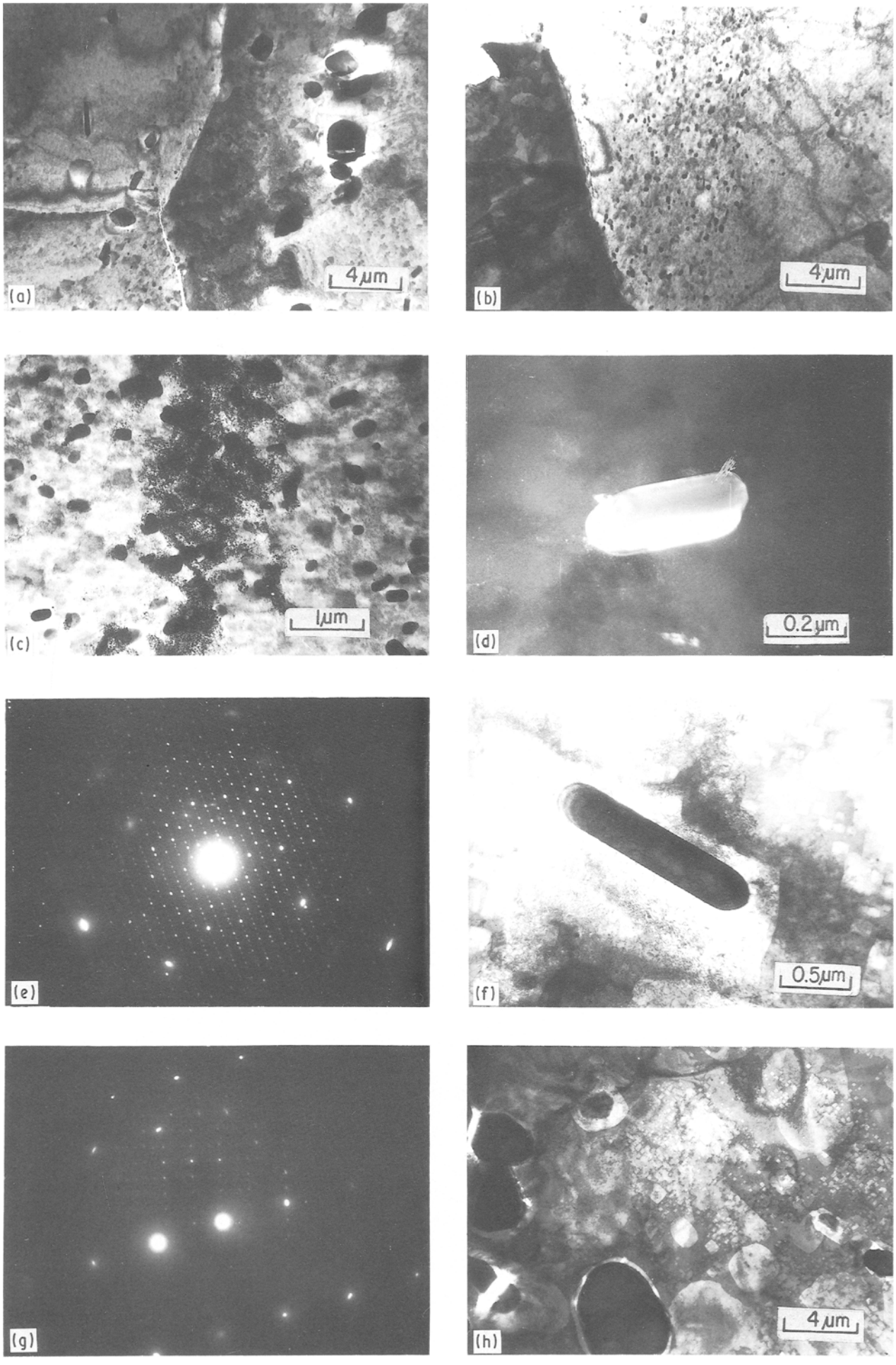

Figure 10a–h

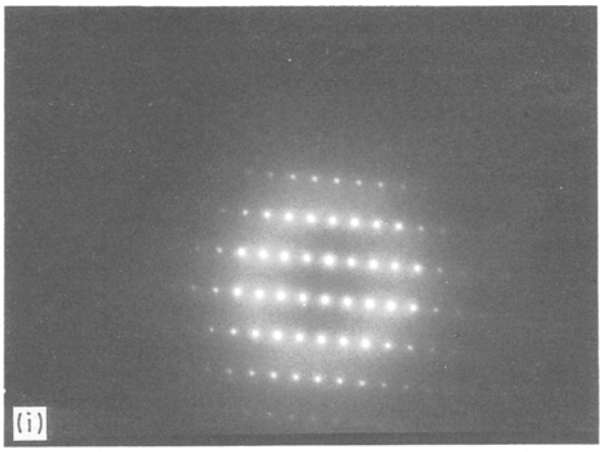

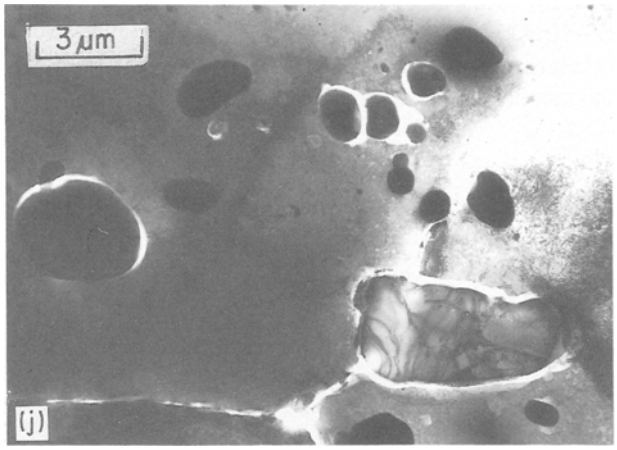

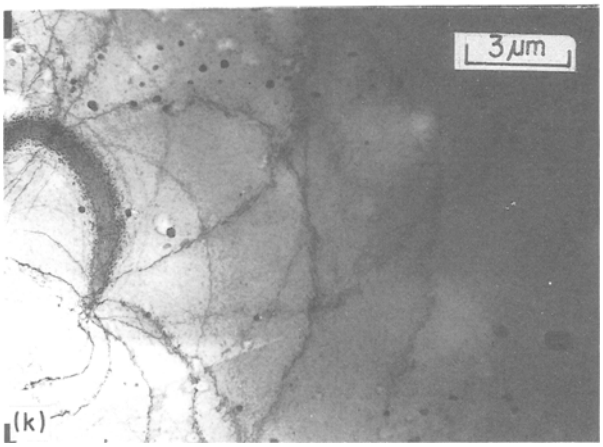

Figure 10 Electron micrographs of aged specimens at 423 K for different times and tensile tested at a strain rate of $5.56 \times 10^{-5}\,s^{-1}$ at 293 K. (a–e) For samples aged 1 h: (a) coarse and fine precipitates of $MnAl_6$, (b, c) fine precipitates of Mg_2Al_3, (d) dark-field and (e) diffraction pattern of Mg_2Al_3 present in (c). (f, g) Aged 6 h: (f) rod-shaped Mg_2Al_3 is present, (g) the diffraction pattern from it. (h, i) Aged 10 h: (h) large precipitates of $MnAl_6$ are present, (i) the diffraction pattern from it. (j, k) Aged 20 h: the presence of (j) coarse precipitates of $MnAl_6$ along the grain boundaries as well as in the aluminium matrix, (k) fine precipitates of Mg_2Al_3.

material at 423 and 473 K, and tensile tested material at room temperature (293 K) at a strain rate of $5.56 \times 10^{-5}\,s^{-1}$, three regions could be discerned.

In the 1–10 h range, ductility and strength increase with time, to a maximum. Electron microscopic investigations of the microstructure of material aged for 1 h at 423 and 473 K (Table II), revealed the presence of coarse precipitates of $MnAl_6$ (Figs 10a and 11b) and fine precipitates of Mg_2Al_3 (Fig. 10b–d). Thus the changes in properties observed in the tensile tests have to be understood in terms of precipitation which takes place in the starting material and that formed during isothermal ageing. The major impurities in the present material were (wt %) 5.8% Mg, 0.5% Mn, 0.4% Fe and 0.4% Si. In the fcc aluminium solid solution, the maximum solubility of magnesium in aluminium is 17.36 wt % (18.90 at %) at a eutectic temperature of 723 K [16]. On the other hand, the maximum solubility of manganese in aluminium is 1.25 wt % (0.62 at %) at a eutectic temperature 931 K [17]. Thus the total

TABLE II : Structural changes in isothermal aged specimens of Al–5.8% Mg alloy of grain size 25 μm and tensile tested at a strain rate of $5.56 \times 10^{-5}\,s^{-1}$ at 293 K (Figs 1–5)

Ageing time (h)	Ageing temperature	
	423 K, Fig. 10a–k	473 K, Fig. 11a–i
1	Fig. 10a shows the presence of coarse and fine precipitates of $MnAl_6$, while fine precipitated particles of Mg_2Al_3 are present in Fig. 10a–d. Fig. 10d and e are the dark-field and diffraction pattern of the second-phase particles of Mg_2Al_3 present in Fig. 10c, respectively, from which $a = 2.802$ nm could be calculated.	Fig. 11a shows the presence of sub-grain boundaries and fine precipitates of Mg_2Al_3. From the X-ray analysis produced in the microscope (Fig. 11c), it could be concluded that the coarse precipitates of $MnAl_6$ present in Fig. 11b contain Mn in addition to Al.
6	A rod-like precipitated particle of Mg_2Al_3 is shown in Fig. 10f and Fig. 10g is the diffraction pattern from it.	
10	In this stage of ageing (10 h), precipitates of $MnAl_6$ have increased in size (Fig. 10h) compared with those present in a specimen aged for 1 h (Fig. 10a), and Fig. 10i is the diffraction pattern from it.	Precipitated particles of Mg_2Al_3 have been grown by increasing the ageing time as shown in Fig. 11d, compared with Fig. 11a. Sub-grain boundaries are still present (Fig. 11d and e). At the same time, a new phase particle was seen in this stage (Fig. 11e), and Fig. 11f is the diffraction pattern from it, from which $a = 1.04$ nm could be calculated.
20	Fig. 10j shows the presence of coarse precipitates of $MnAl_6$ along the grain boundaries, as well as in the Al matrix, while fine precipitates of Mg_2Al_3 are present, as shown in Fig. 10k.	Different shapes of the same type of precipitates present in Fig. 11e are seen in Fig. 11g, and Fig. 11 h is the diffraction pattern from it. On the other hand, large precipitates of $MnAl_6$ were seen in some areas of the sample (Fig. 11i).

amount of manganese should have been precipitated as $MnAl_6$ even during solidification. It has to be emphasized in this connection that the size of the second-phase particles produced during solidification is of the order of 1–10 μm [18–20]. From the X-ray analysis (Fig. 11c) of the large precipitates present in Fig. 11b, and the diffraction pattern in Fig. 10i for the coarse precipitates present in Fig. 10h, the presence of $MnAl_6$ precipitates with size 1.64–2.00 μm could be established. Moreover, these precipitates were distributed non-uniformly. The presence of Mg_2Al_3 and $MnAl_6$ precipitates in the present work, is also consistent with those reported earlier [10, 11, 21]. It was also observed that, the dislocation and subgrains were

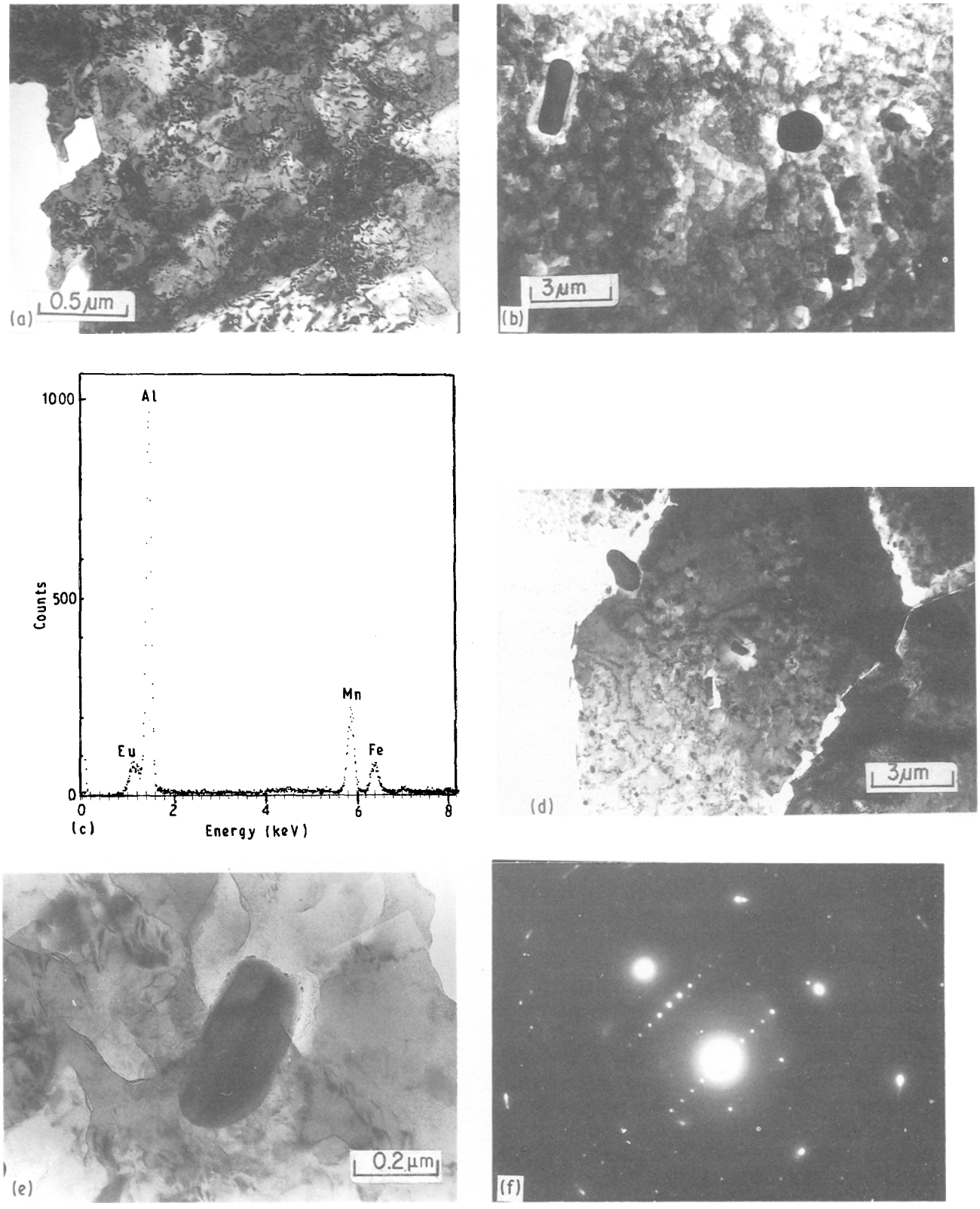

Figure 11a–f

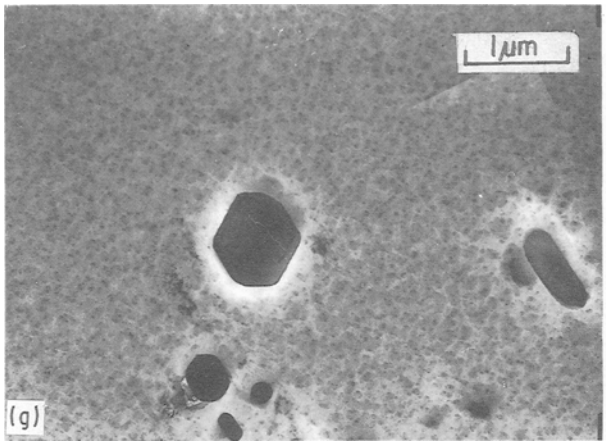

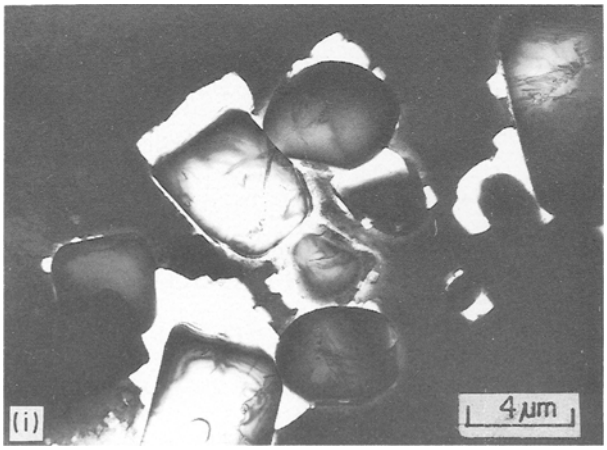

Figure 11 Electron micrographs of specimens aged at 473 K, for different times and tested at a strain rate of $5.56 \times 10^{-5}\,s^{-1}$ at 293 K. (a–c) Aged specimens for 1 h, showing the presence of: (a) sub-grain boundaries and fine precipitates of Mg_2Al_3: (b) coarse precipitates of $MnAl_6$, and (c) the X-ray analysis of $MnAl_6$ present in (b). (d–f) Aged 10 h: showing the presence of: (d) fine precipitates of Mg_2Al_3 and one coarse particle of $MnAl_6$, (e) sub-grain boundaries and precipitated particles of ε-$Mg_{23}Al_{30}$, (f) the diffraction pattern from it. (g–i) Aged at 20 h: (g) different shapes of precipitates of ε - $Mg_{23}Al_{30}$ phase, (h) the diffraction pattern from it; (i) large precipitated particles of $MnAl_6$ are present.

pinned by the precipitates. This proved that the precipitated particles cause disruption of flow and their presence led to an increase in strength.

In the range 10–20 h, the observed drop in ductility due to precipitation should be accompanied by an increase in yield strength [11, 22]. As coarsening of precipitates leads to a decrease in the effectiveness of precipitation hardening [22], the effect of ageing time on the size of the precipitates, should also contribute to the shape of the strength–time plots. Naturally, an increase in the ageing time will provide a chance for solute diffusion and facilitates the coarsening of the precipitates. On the other hand, from the relation [23], $\tau = Gb/d$, where G is the shear modulus, b Burger's vector and d is the distance between particles, the stress to expand the dislocation past particles increases as the distance between particles decreases. It can also explain why the strength and work hardening increase in the time range 1–10 h where the precipitates are fine and the coarsening of the precipitates and the attendant decrease in their number at still longer time, will lead to a decrease in strength.

On the other hand, electron microscopic investigations of specimens aged at 473 K for 10 and 25 h, revealed that, in addition to the presence of Mg_2Al_3 and $MnAl_6$ precipitates (Fig. 11d and i), a new phase with different shapes and $a = 1.04$ nm, has been detected (Fig. 11e and g). That is consistent with ε-$Mg_{23}Al_{30}$ structure, having a rhombohedral unit cell a-1.033 nm, and its structure closely resembles that of the R phase [24]. Accordingly, the presence of ε-phase in addition to the continuing presence of coarse and fine precipitates of $MnAl_6$ and Mg_2Al_3 (Figs 10j, k and 11i), led to an increase in yield and ultimate tensile strength, flow stress and work hardening exponent beyond the ageing time of 25 h (Figs 1, 2, 4a, b, 5 and 7). On the other hand, it is consistent with the presence of double peaks of hardness versus ageing time of aged Al–16% Ag alloy at 433 K [25] and Al–Cu alloy aged at 403 K [26].

Moreover, the observation of Davenport and Bain [27], that the coarsening of fine precipitates is responsible for the ultimate decrease in the strength of an age-hardenable alloy, is in agreement with the present findings, that the strength of the material decreases with increasing ageing temperature.

From the parabolic stress–strain relation [2, 9], the σ versus $\varepsilon^{1/2}$ curves could be divided into two linear parts (Fig. 8) which are very similar with those reported earlier [2, 5, 6, 9–11, 28].

The results of studies on the effect of different degrees of deformation on the recrystallization temperature of Al–5.8% Mg alloy (Fig. 9), gave curves showing a peak recovery at 375 K, which from the other point of view, is consistent with 0.2% yield stress, ultimate tensile strength, flow stress and work hardening exponent versus ageing time curves (Figs 1, 2, 5 and 7), due to the presence of $MnAl_6$ and Mg_2Al_3 precipitates (Table II). On the other hand, the recrystallization temperature decreases with deformation, as is conventionally known [29].

5. Conclusions

The present studies on the correlation between the mechanical properties and microstructural changes of aged Al–5.8% Mg alloy at 423 and 473 K led to the following conclusions.

1. The general behaviour curves of 0.2% yield strength, ultimate tensile strength, flow stress and work hardening exponent, n, versus ageing time is the same in both cases. The strength and ductility increase with time, reach maximum value and then decrease to a minimum, followed by an increase beyond an ageing time of 25 h.

2. Electron microscopic investigations revealed that: (a) the increase in strength and work hardening exponent, n, to maximum at 10 h, and the drop in ductility in the time range 10–25 h are attributed to the precipitation of $MnAl_6$ and Mg_2Al_3; (b) as coarsening of precipitates leads to a decrease in the effectiveness of precipitation hardening, and the stress to expand the dislocation past particles increases as the distance between particles decreases, it can be concluded that the increase in strength up to maximum at 10 h, where the precipitates are fine, and coarsening of the precipitates and the attendant decrease in their number beyond 10 h, led to the decrease in the strength up to 25 h; (c) the increase in strength beyond an ageing time of 25 h is due to the continuing presence and precipitation of $MnAl_6$ and Mg_2Al_3, in addition to the precipitation and appearance of different shaped particles of ε-$Mg_{23}Al_{30}$ phase.

3. The yield and ultimate tensile strength, flow stress and work hardening exponent, n, decrease with increasing ageing temperature.

4. From the parabolic stress–strain relation, the σ versus $\varepsilon^{1/2}$ curves could be divided into two linear parts.

5. The Brinell hardness increases and the recrystallization temperature decreases with deformation.

Acknowledgements

We thank Dr G. Van Tendeloo, Dr J. Van Landuyt, F. Schallenberg and the Electron Microscope Group, University of Antwerp, Belgium, for the facilities granted and their help in the electron microscopic work at Belgium. We also thank Dr Mansour Khaalf, Head, Physics and Material Science Department, for encouragement and interest in this work.

References

1. C. A. PAMPILO, H. BILONI and D. E. EMBURY, "Aluminium Transformation Technology and Applications", Materials/Metalworking Technology Series, (ASM, Metals Park, Ohio, 1978) p. 214.
2. A. M. HAMMAD, K. A. PADMANABHAN and T. R. ANANTHARAMAN, *Trans. Ind. Inst. Metals* **30** (1977) 327.
3. A. M. HAMMAD, K. A. PADMANABHAN, G. V. TENDELOO and T. R. ANANTHARAMAN, *ibid.* **30** (1977) 338.
4. A. M. HAMMAD, K. A. PADMANABHAN and T. R. ANANTHARAMAN, *J. Mater. Sci.* **15** (1980) 2136.
5. A. M. HAMMAD, K. A. PADMANABHAN, G. V. TENDELOO and T. R. ANANTHARAMAN, *Z. Metallkde* **78** (1987) 103.
6. *Idem, ibid.* **78** (1987) 113.
7. A. M. HAMMAD, *Trans. Ind. Inst. Metals* **40** (1987) 39.
8. *Idem, ibid.* **40** (1987) 423.
9. A. M. HAMMAD, K. K. RAMADAN and M. A. NASR, *Z. Metallkde* **80** (1989) 173.
10. A. M. HAMMAD and K. K. RAMADAN, *ibid.* **80** (1989) 178.
11. *Idem, ibid.* **80** (1989) 431.
12. I. A. EL-SHANSHOURY, I. M. VORONIN and M. S. ABDEL-AZIM, *J. Nucl. Mater.* **29** (1969) 161.
13. I. A. EL-SHANSHOURY and F. I. GADALLAH, *ibid.* **36** (1970) 87.
14. I. A. EL-SHANSHOURY, F. I. GADALLAH and A. M. HAMMAD, *ibid.* **42** (1972) 203.
15. P. LUDWIK, "Elemente der Technologischen Mechanik" (Springer, Berlin, 1960).
16. J. L. MURRAY, *Bull. Phase Diagrams* **3** (1) (1982).
17. E. H. DIX, W. L. FINK and L. A. WILLEY, *Trans. AIME* **104** (1933) 335.
18. T. H. MULHERIN and H. ROSENTHAL, *Metal. Trans.* **2** (1971) 427.
19. C. J. PEEL, R. N. WILSON and P. J. E. FORSTH. *J. Metal Sci.*, **6** (1972) 102.
20. S. M. EL-SOUDANI and R. M. PELLOUX, *Metallogr.* **6** (1973) 37.
21. A. M. HAMMAD and O. A. RUGEBANI, *J. High. Temp. Technol.* **8** (1990) 261.
22. J. W. MARTIN, "Precipitation Hardening" (Pergamon, Oxford, 1968) p. 29.
23. P. G. SHEWMON, "Transformation in Metals" (McGraw-Hill, New York, 1969) p. 311.
24. M. H. MUELLER and H. W. KNOTT, *Trans. Met. Soc. AIME* **227** (1963) 674.
25. R. NICHOLSON and J. NUTTING, *Acta Metall.* **9** (1961) 332.
26. T. HEAL and H. HARDY, *J. Inst. Metals* **82** (1953–1954) 239.
27. E. D. DAVENPORT and E. BAIN, *Trans. Amer. Soc. Metals* **32** (1935) 1047.
28. N. HANSEN, *Acta Metall.* **18** (1970) 137.
29. I. A. EL-SHANSHOURY, I. M. VORONIN, F. I. GADALLAH, A. M. HAMMAD and H. G. MOHAMED, in "Proceedings of the IAEA Conference on Radiation Damage in Reactor Materials", Vienna, IAEA SM-120/C-4, 1 (1969) p. 249.

Received 2 August 1990
and accepted 12 February 1991